**SANDIA REPORT**
SAND2000-1614
Unlimited Release
Printed July 2000

# Changes in the Nonlinear Viscoelasticity of Carbon Black Filled Rubber as it Ages

Douglas Adolf and Wei-Yang Lu

Prepared by
Sandia National Laboratories
Albuquerque, New Mexico 87185 and Livermore, California 94550

Sandia is a multiprogram laboratory operated by Sandia Corporation, a Lockheed Martin Company, for the United States Department of Energy under Contract DE-AC04-94AL85000.

Sandia National Laboratories

Issued by Sandia National Laboratories, operated for the United States Department of Energy by Sandia Corporation.



SAND 2000-1614
Unlimited Release
Printed July 2000

# Changes in the Nonlinear Viscoelasticity of Carbon Black Filled Rubber as it Ages

Douglas Adolf, Organic Materials Department
Wei-Yang Lu, Materials Mechanics Department
Sandia National Laboratories
P.O. Box 5342
Albuquerque, NM 87185

## Abstract

The effects of chemical aging on the behavior of carbon black filled rubber were investigated by two types of tests, aging under no strain and aging under a constant strain. A slight modification of the damage-based theory of Segalman, used previously on unaged samples, was found to be consistent with the experimental data.

# I. INTRODUCTION

*Project History and Goals*

In the first interactions between Goodyear and Sandia, our goal of accurately computing rolling resistance required us to develop a viscoelastic representation of carbon black filled rubber that captured dissipation correctly in these highly nonlinear materials. As earlier studies suggested,[1] we proposed that a BKZ formalism[2] might be appropriate and proceeded to assess its validity. To strains of 10%, we found that a separable BKZ model captured step strain, oscillatory strain, multiaxial oscillatory strain, and multimodal oscillatory strain tests fairly well.[3]

We had also been tasked to investigate the behavior of green rubber for predicting stresses during mold filling and cure. Even though mold filling may involve relatively large local strains, the average global strains are much lower and we limited our investigations to strains of no more than 25%. In this regime for green rubber, we found that BKZ again performed well in step strain, advancing double step strain, and oscillatory strain tests.[4] Under reversing double step strain, the Wagner modification performed better, which has been observed for other materials as well.[5] We subsequently tracked the evolution of the nonlinear viscoelasticity from the green state through cure. While the strain and time dependencies were still observed to be separable, the spectrum of relaxation times did change as cure progressed.[3] This appeared quite computationally cumbersome at the time. We will show a simpler resolution to this problem later in this paper.

In the course of these studies, we realized that even though BKZ may

be capturing observed phenomena accurately it is intrinsically an integral formalism and does not possess a differential analog. Since a differential model would be much more computationally efficient, Dan Segalman created a similar though not identical damage-based differential model which reproduced both the experimental data and the BKZ predictions fairly well.[6]

In this present study, we experimentally investigated how the material response changed as it chemically aged as a step toward predicting tire durability. Since the regions deep within a tire are essentially anerobic, this study focused on aging in the absence of oxygen. This proved to be a more difficult requirement than originally anticipated. We then examined how these experimental results affected the damage-based constitutive formalism.

*BKZ Constitutive Equation*

We adopted the simplest version of the BKZ formalism, a separable model employing the infinitesimal strain measure. Since the onset of nonlinearities for these carbon black filled rubbers occurs at extremely low strains (~$10^{-3}$), significant strain softening can occur by a strain of 10% and yet we can still reasonably apply an infinitesimal strain measure. For a shearing deformation of these nearly incompressible materials, the first strain invariant is almost constant, so the observed strain softening must arise from a dependence of the work function on the second invariant. The BKZ formalism thus reduces to

$$\underline{\underline{\sigma}} = -P\,\underline{\underline{I}} + \int_{-\infty}^{t} ds\, m(t^* - s^*)\, h(I_2(t) - I_2(s)) \left[ \underline{\underline{\gamma}}_{dev}(t) - \underline{\underline{\gamma}}_{dev}(s) \right] + 2G_\infty \underline{\underline{\gamma}}_{dev}(t) \qquad (1)$$

$$\text{where } \underline{\underline{\gamma}}_{dev}(t) = \underline{\underline{\gamma}}(t) - \frac{1}{3}\underline{\underline{I}}\, I_1\left(\underline{\underline{\gamma}}(t)\right)$$

where P is the pressure, m=-dG/dt (G is the shear stress relaxation function), h is the "damping function" that describes the nonlinear strain softening, $\underline{\underline{\gamma}}$ is the infinitesimal strain tensor, $\underline{\underline{I}}$ is the identity tensor, $I_1$ and $I_2$ are the first and second invariants of $\underline{\underline{\gamma}}$, and $G_\infty$ is the rubbery shear modulus. The reduced time, t*, is defined as $t^* = \int_0^t \frac{du}{a(u)}$ where a is the viscoelastic "shift factor" that describes the acceleration of relaxation times with temperature. We have found that the standard WLF shift factor can be used for these filled systems with the WLF parameters, $C_1$ and $C_2$, determined for the analogous unfilled system.[7] For the relatively low strains investigated to this point, the predictions from this simple approach have been satisfactory. However, at higher strains (say greater than 50%), we probably need to employ finite strain measures and address the dependence of the strain softening on the first invariant as well.

*Differential Analog*

Since the BKZ equation does not have a differential form, some assumptions must be made when creating an analogous differential formalism. Segalman has adopted a damage-like approach where the

"strength" of the relaxation mode softens with applied strain. In this fashion, we recover the characteristic vertical shift observed in step strain tests of varying magnitude. And since the "damage" recovers, we predict the observed slow reversal of this softening with time. His formalism can be expressed as

$$\underline{\underline{\sigma}} = -P\,\underline{\underline{I}} + \sum \underline{\underline{\sigma}}_{dev_i} + 2G_\infty \underline{\underline{\gamma}}_{dev}$$

$$\frac{d\underline{\underline{\sigma}}_{dev_i}}{dt} + \frac{\underline{\underline{\sigma}}_{dev_i}}{\tau_i} = 2G_i\, g(d)\, \dot{\underline{\underline{\gamma}}}_{dev} \qquad (2)$$

where $\sum_i G_i = G_{glassy} - G_\infty$ and $\underline{\underline{\gamma}}_{dev} = \underline{\underline{\gamma}} - \frac{1}{3}\left(tr\underline{\underline{\gamma}}\right)\underline{\underline{I}}$

$$d = \sum a_{d_i} d_i$$

$$\frac{d(d_i)}{dt} + \frac{d_i}{\tau_i} = a_{d_i} \left|\dot{\underline{\underline{D}}}\right| \qquad (3)$$

where $\sum_i a_{d_i} = 1$

$$\dot{\underline{\underline{D}}} = \left(\dot{\underline{\underline{\gamma}}}_{dev} : \underline{\underline{N}}\right)\underline{\underline{N}}\; H\left(\dot{\underline{\underline{\gamma}}}_{dev} : \underline{\underline{N}}\right)\; \delta\left(\left|\underline{\underline{\gamma}}_{dev} - \underline{\underline{\gamma}}_K\right| - \gamma_I\right)$$

$$\text{where } \underline{\underline{N}} = \frac{\underline{\underline{\gamma}}_{dev} - \underline{\underline{\gamma}}_K}{\left|\underline{\underline{\gamma}}_{dev} - \underline{\underline{\gamma}}_K\right|} \qquad (4)$$

$$\underline{\underline{\gamma}}_K = \sum a_{K_i} \underline{\underline{\gamma}}_{K_i}$$

$$\frac{d\underline{\underline{\gamma}}_{K_i}}{dt} + \frac{\underline{\underline{\gamma}}_{K_i}}{\tau_i} = a_{K_i}\left[\frac{\underline{\underline{\gamma}}_{dev}}{\tau_i} + (1-\beta)\,\dot{\underline{\underline{D}}}\, H(\dot{\underline{\underline{D}}})\right] \qquad (5)$$

where $\sum_i a_{K_i} = 1$

$$\underline{\underline{\gamma}}_I = \sum a_{I_i} \underline{\underline{\gamma}}_{I_i}$$

$$\frac{d\underline{\underline{\gamma}}_{I_i}}{dt} + \frac{\underline{\underline{\gamma}}_{I_i}}{\tau_i} = a_{I_i} \beta \left| \dot{\underline{\underline{D}}} \right| \qquad (6)$$

where $\sum_i a_{I_i} = 1$

where H is the Heaviside function and $\delta$ is the delta function.

While these equations appear imposing, they actually present a simple physical picture. In Eq.2, the function, g, furnishes the required strain softening; g=1 for small damage and decreases as damage increases. In Eq. 3, we see that the partial damages, $d_i$, increase with the tensorial damage rate, $\dot{D}$, and recover with the linear viscoelastic relaxation spectrum. Eq. 4 defines the damage rate such that it increases only when we are outside the damage surface itself defined by isotropic, $\gamma_I$, and kinematic, $\gamma_k$, contributions in Eq. 5 and 6. $\beta$ is the partitioning coefficient between these two contributions.

Since this damage-based constitutive model was not constructed from a strain energy, however, it is not guaranteed to be thermodynamically consistent. This should not imply that the model is necessarily inconsistent, but we must keep this fact in the back of our minds for future reference.

## II. AGING PROTOCOL

### *Procedure*

The materials used in this study were natural rubber filled with 18vol% carbon black and were identical to those used in the previous

studies with Goodyear. Therefore, we should be able to assess the effects of chemical aging on the viscoelastic formalism without confusion from intrinsic material differences.

We agreed that samples would be aged at two temperatures, 100 and 120C, for one month in the absence of oxygen. We tried two different methods to create an anaerobic environment. In the first, we simply evacuated a heated vacuum oven to 15 Torr and aged the samples. We observed that, over time, an oily film appeared on the oven door leading us to worry that the loss of this substance may affect the observed sample "hardness". Therefore, we repeated the aging under nitrogen. In this aging protocol, we evacuated the heated oven to 15 Torr, backfilled with pure ($<10^{-5}$% oxygen) bottled nitrogen, and repeated this procedure twice more. Both procedures resulted in similar aging behavior, although both may be insufficiently anaerobic as described later.

There is a coupling between chemistry and mechanical response that requires us to perform at least two different types of mechanical aging tests. Let's assume that the chemistry relates to the formation or scission of crosslinks. If our sample is simply sitting in the heated oven under no strain, the new crosslinks will be formed in the unstrained state. When we then take that sample out of the oven, apply a strain, and measure its response, those new crosslinks will tend to increase the sample's equilibrium modulus while the old crosslinks that were broken will decrease the equilibrium modulus. Since this modulus is proportional to the total number of crosslinks at the test time, we will be unable to distinguish between the rates of scission or formation.

However, if our sample is aged under a constant strain as it sits in the heated oven, a different picture emerges. As crosslinks are broken, the stress required to maintain the constant strain will decrease. New

crosslinks, however, will be inserted into an unstrained state at this constant strain and will therefore not contribute to the stress. As we periodically take our sample out of the oven and measure the stress required to maintain the constant strain, we will be sensitive to only those crosslinks which have broken. By examining both of these tests, we are now able to distinguish between the rates of crosslink formation and scission. These are the two types of tests that we performed to assess the validity of any proposed nonlinear viscoelastic constitutive formalism.

*Observed Difficulties*

As stated above, difficulties were observed in the aging protocol. In particular, our sample's linear viscoelastic modulus initially decreased by a slight amount over a period of days, but subsequently increased by roughly a factor of two over a period of weeks. These results are in contrast to those for samples extracted from deep within tires where we are almost assured of an absence of oxygen. In these samples, Goodyear invariably observes a monotonic decrease in modulus with increased aging; their samples decrease by roughly 20% over a month's time.

Goodyear was suspicious that these differences indicated oxidative aging in our oven-aged samples. As such, they sectioned these oven-aged samples and measured the micro-hardness along the cross-section. If oxidative aging were present, one would anticipate that the older samples would show a nonuniform cross-sectional microhardness, with the outside being harder than the inside. In Fig. 1 provided by Goodyear, this suspicion is confirmed. Here we see that the unaged sample as well as those samples aged 1 and 4 days are fairly uniform in cross-sectional hardness. These are the samples which also exhibited a lower macroscopically measured modulus. In contrast, those samples aged 15 and 30 days show a markedly

harder surface most probably due to oxidative aging. These samples also exhibited macroscopic hardening with age.

Two conclusions might be made from these observations. First, achieving truly anaerobic aging under laboratory conditions is more challenging than one might think, and second, a little bit of oxygen goes a long way in inducing hardening. Both of these observations are consistent with those of Gillen in his dynamic aging activities under this CRADA. However, it has not been definitively proven that these differences are indisputably due to the presence of a small amount of oxygen; this is simply our working hypothesis. Fortunately, since our goal was to understand the phenomenology of chemical aging and its affect on some proposed constitutive law, this partial oxidation is not catastrophic. We are still able to quantify the observed behavior and deduce the changes required to a constitutive formalism without understanding the precise chemistry (e.g. oxidative vs. anaerobic). However, from these tests, we are unable to unambiguously decouple the formation and scission reaction rates. This decoupling must be pursued under much more rigorous conditions.

## III. AGING UNDER NO STRAIN

*Test Data*

To reiterate, our first studies considered the effect of chemical aging under no applied strain. Here, the resultant moduli will be sensitive to the total crosslink density, considering both new crosslinks formed and existing ones broken. The samples were aged at 120C for one month. Samples were removed from the aging oven at 1, 4, 15, and 30 days, and the linear dynamic shear moduli were measured in torsion rectangular geometry (2"x1/2"x1/8") with a Rheometrics RMS800 at 30C to evaluate

the effect of aging on the linear viscoelastic relaxation spectrum. The resulting dynamic moduli are shown in Fig. 2. It is clear that the curves can be superposed by vertical shifts indicating that the relaxation spectra are unaffected by aging.

We now need to understand the effect of aging on strain softening, which could be represented by the damping function in the BKZ formalism. The most unambiguous tests for examining strain softening are step strains of varying magnitude. Samples were again aged at 120C and removed at 1, 4, 15, and 30 days. These samples were tested in tension at 30, 70, and 120C at step strains of 5, 20, and 60%. The data are shown in Figs. 3-7. Some chemical degradation is seen at the highest temperatures at Day 0. Beyond this isolated instance, though, all curves can be superposed, which supports the separable BKZ formalism and allows us to extract the damping function. We show the damping function from these tensile tests on aged samples in Fig. 8 and compare it to the damping functions previously determined for both green and cured rubber. The aged damping functions fall right into line with the previous results and do not change with aging chemistry.

That the damping function is unaffected by chemical aging is consistent with the lore of carbon black filled rubbers. It has been claimed that, while the viscoelastic nature is due to the natural rubber itself, the strain softening is thought to arise from the carbon black.[8-12] Since the chemistry most likely occurs in the rubber as a change in crosslink density, the lore would predict that the damping function is independent of aging.

Due to fixturing concerns, it is difficult to perform tensile step strain tests at strains much less than 5%. To assess the damping function at these lower strains, it is convenient to return to shear and perform the historical Payne-type test in which an oscillatory strain is applied of a given

Fig. 1

Modulus Profile

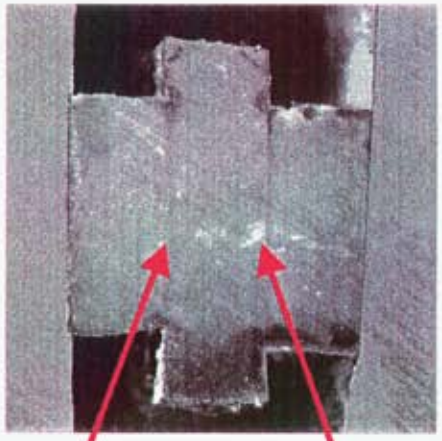

Material aged at Sandia after vacuum and nitrogen backfill

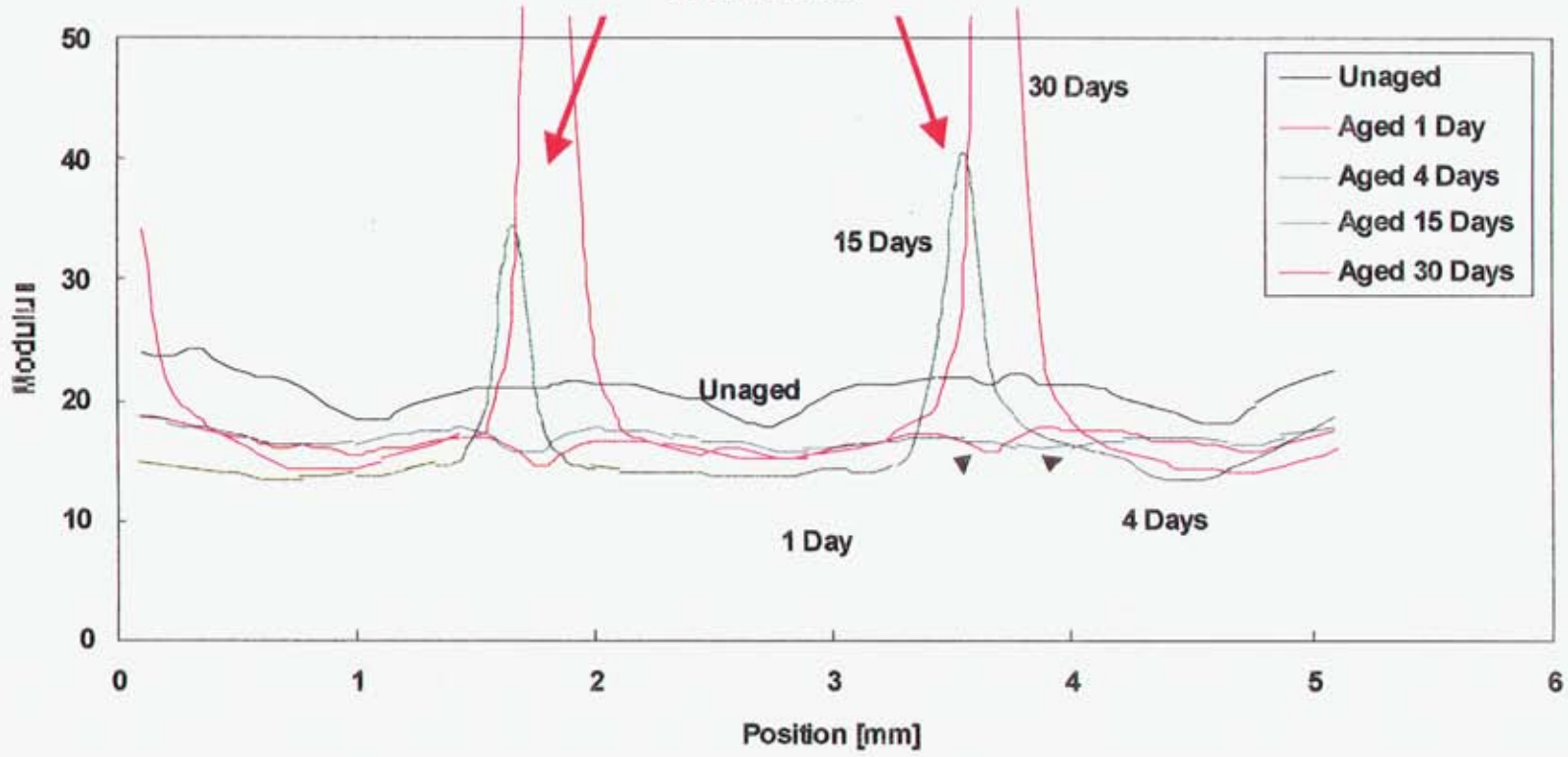

Fig. 2

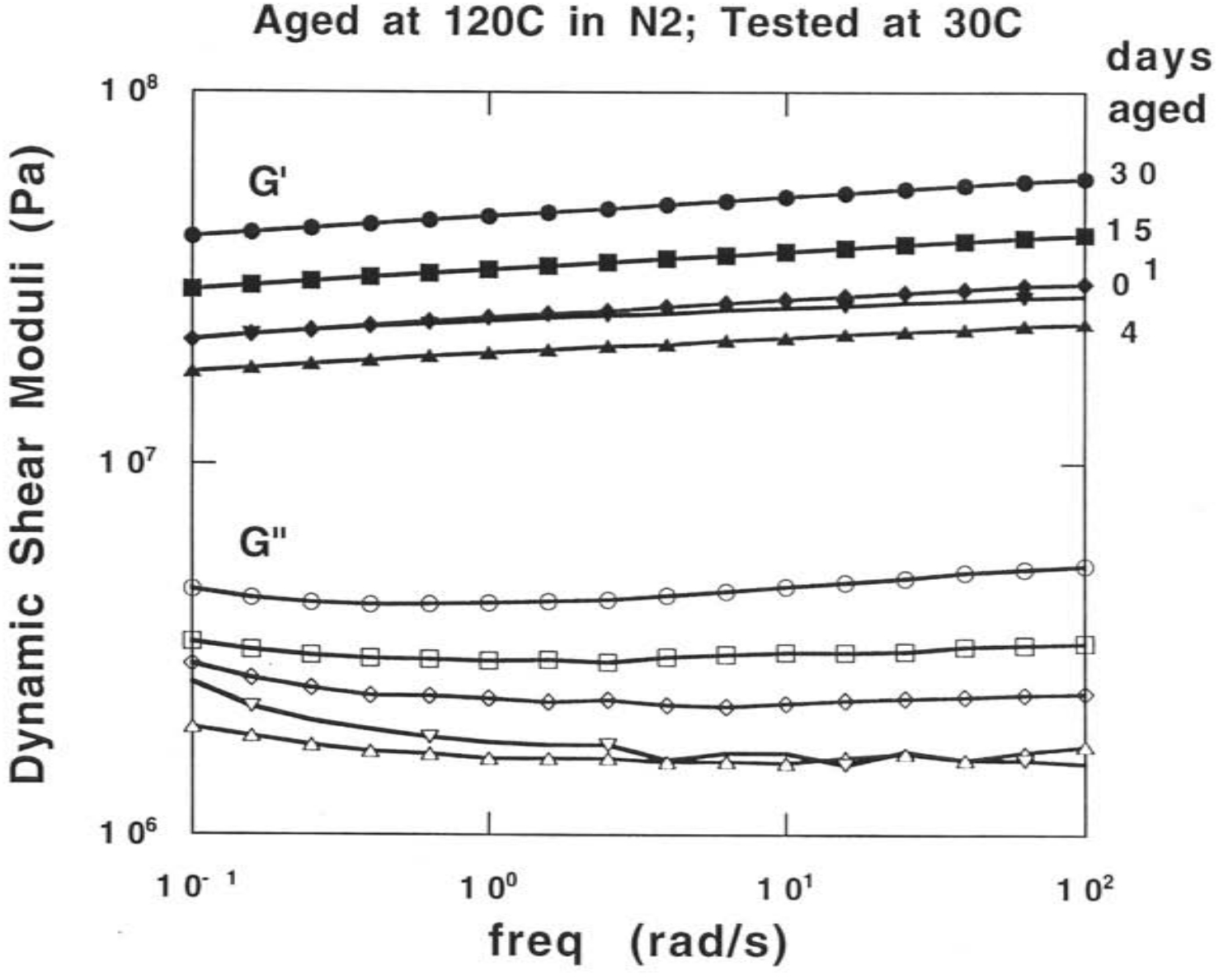
Aged at 120C in N2; Tested at 30C
days aged
30
15
01
4
G'
G"
Dynamic Shear Moduli (Pa)
10^8
10^7
10^6
10^-1
10^0
10^1
10^2
freq (rad/s)

Fig. 3

# 772, 120°C, day 0

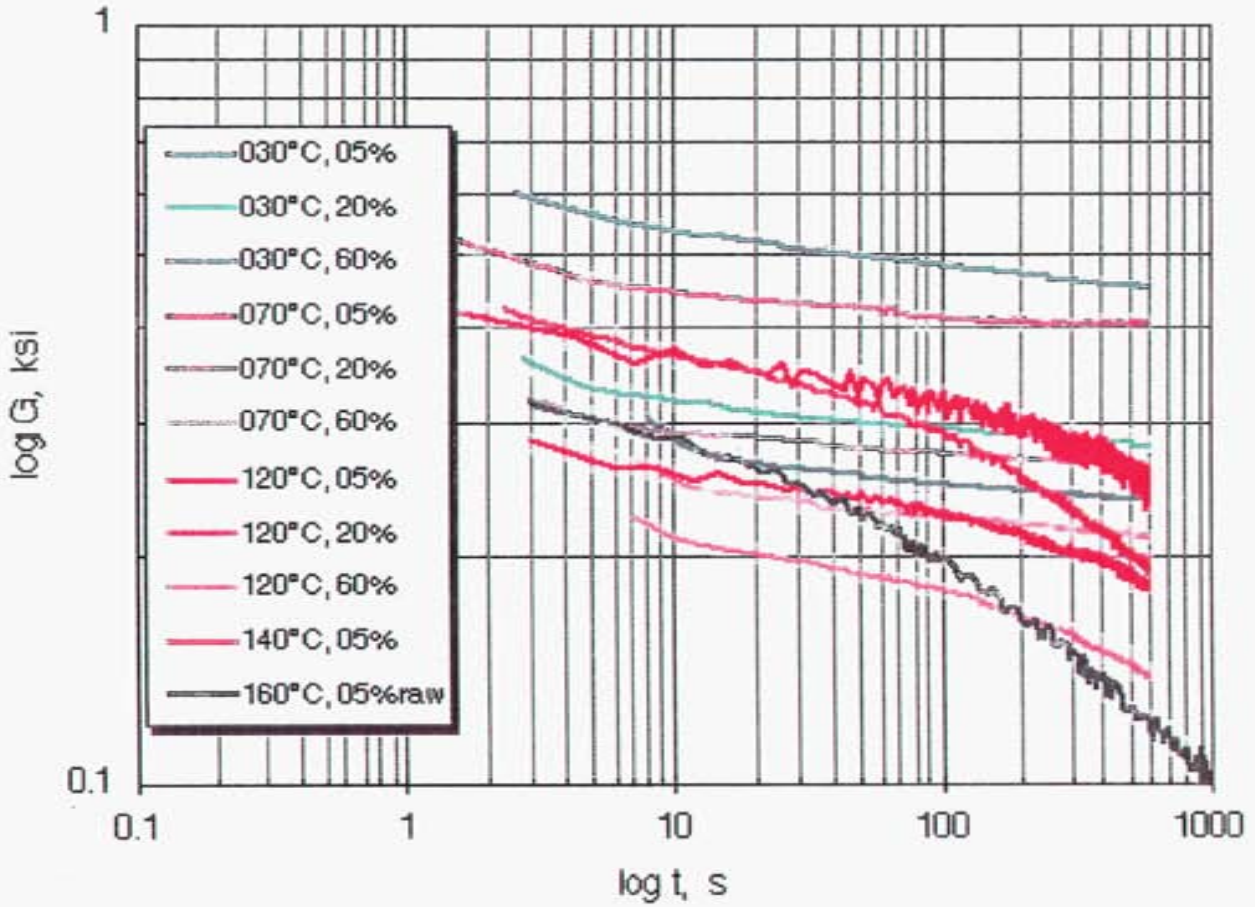

Fig. 4

# 772, 120°C, day 1

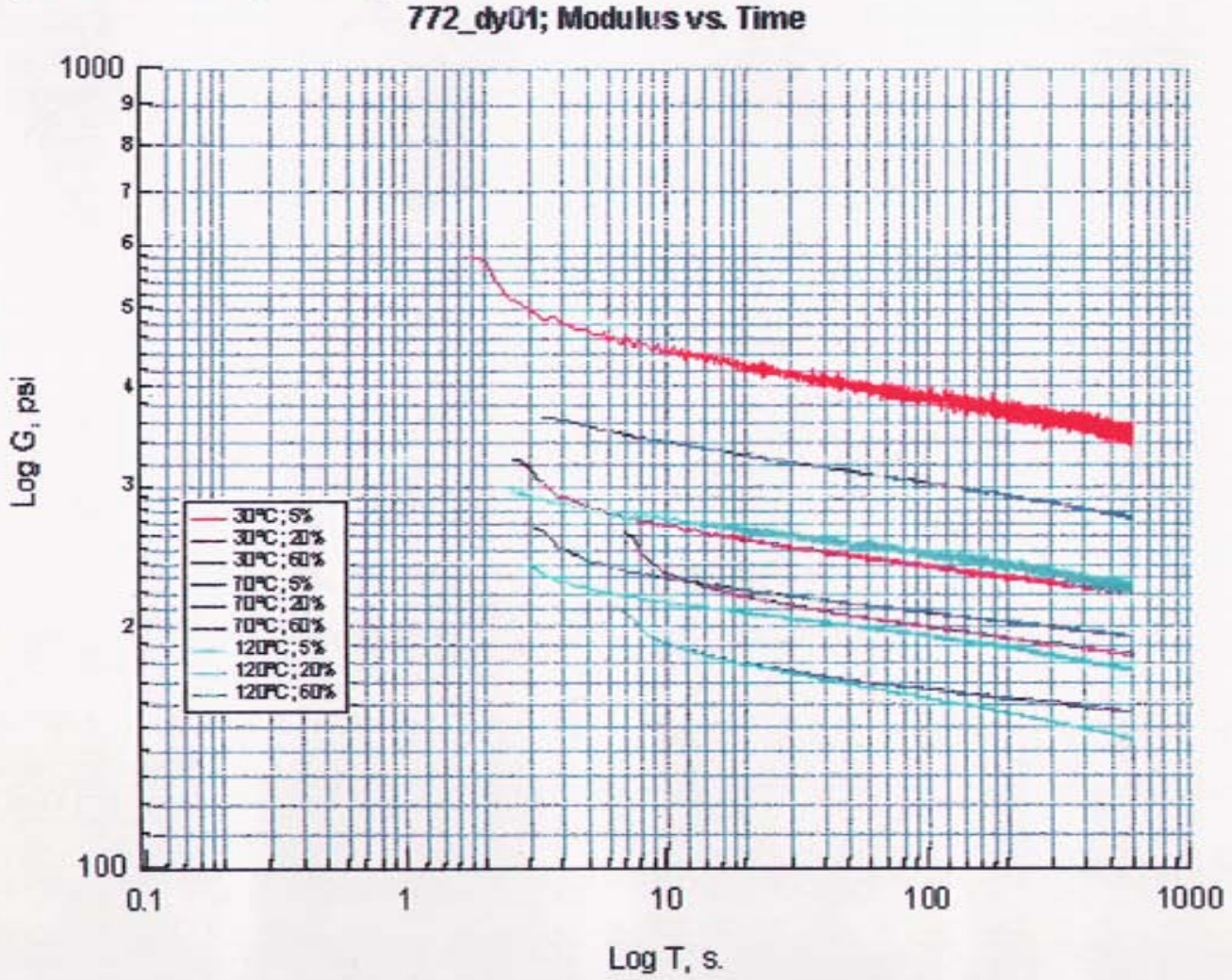

# 772, 120°C, day 4

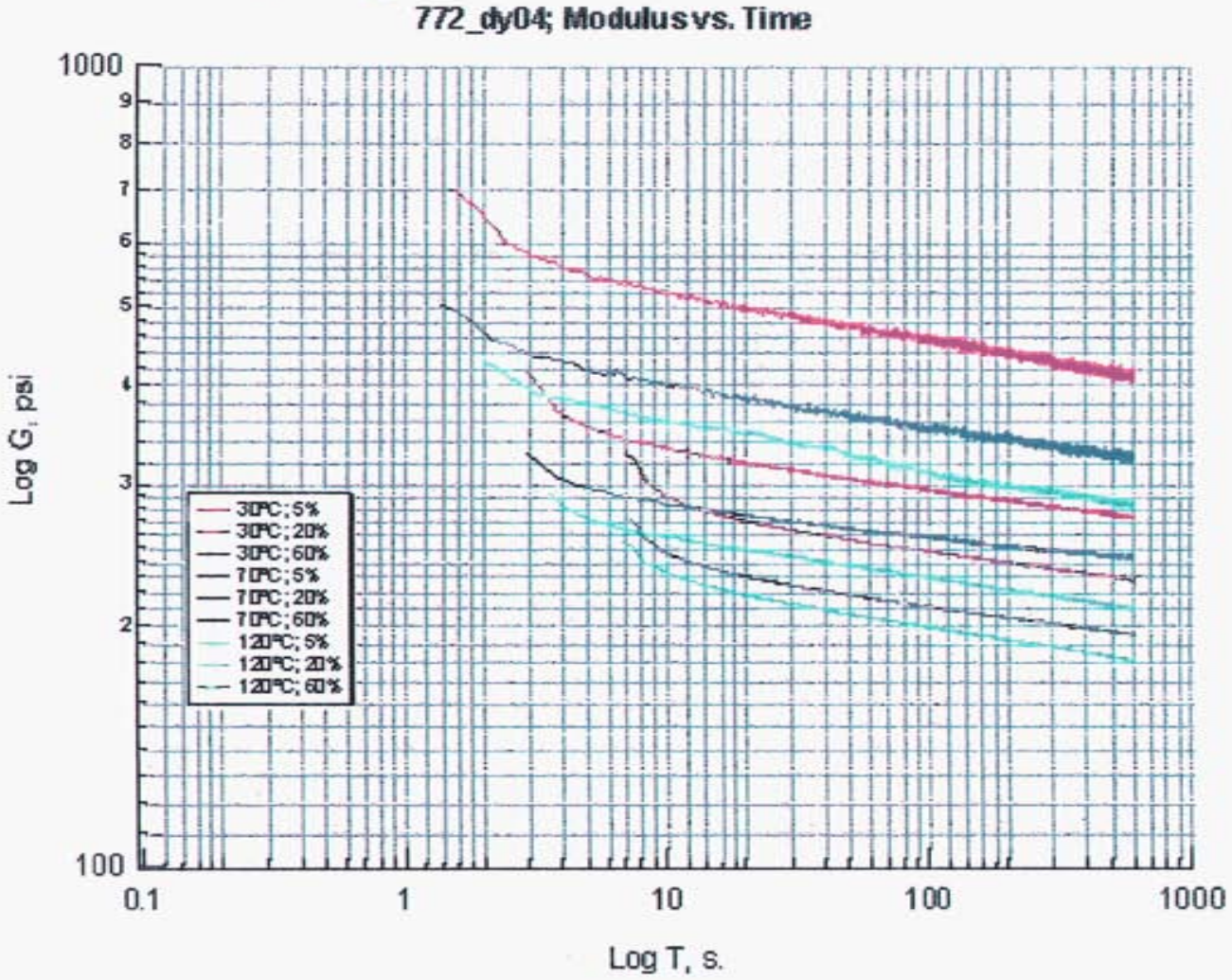

Fig. 6

# 772, 120°C, day 15

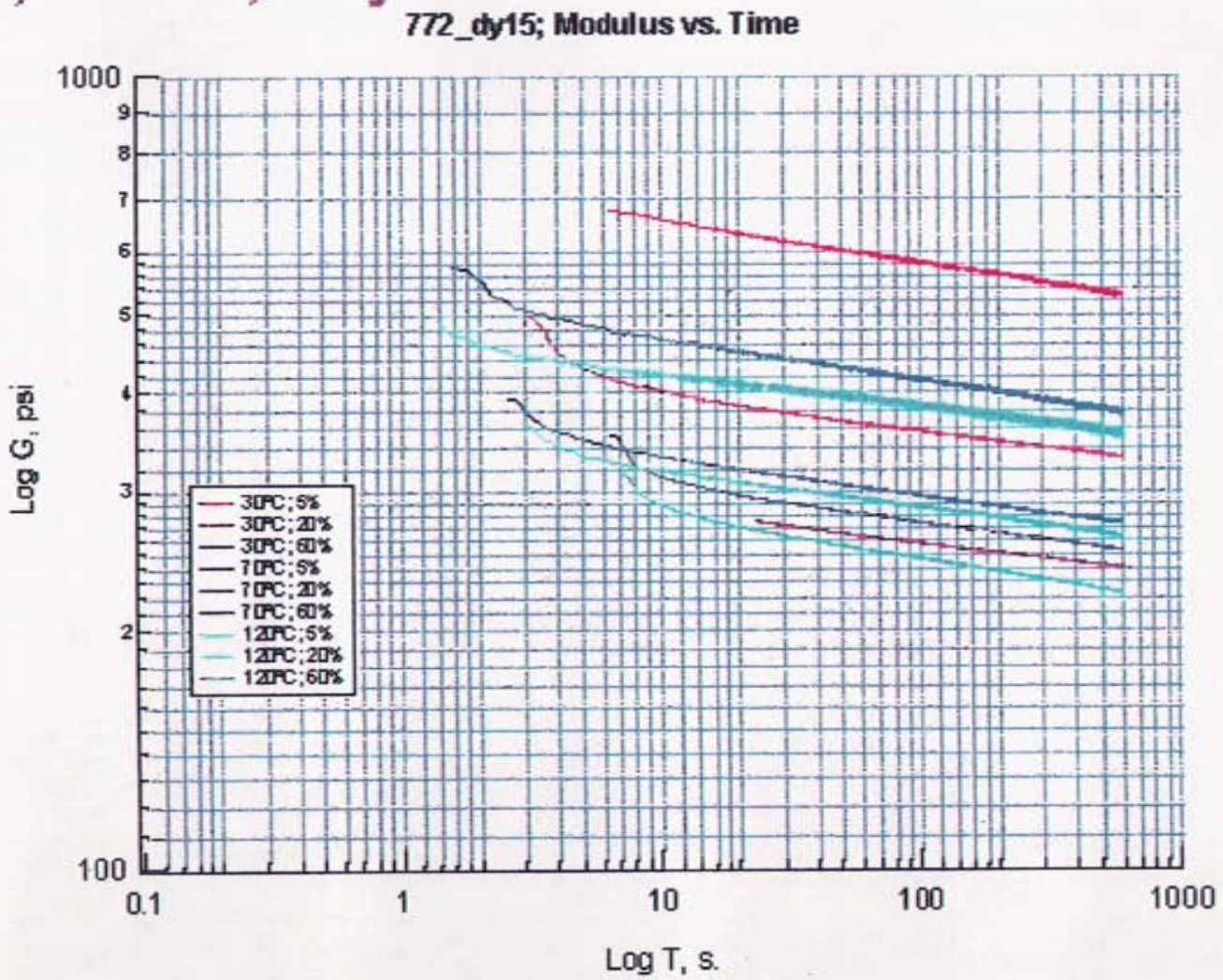

# 772, 120°C, day 30

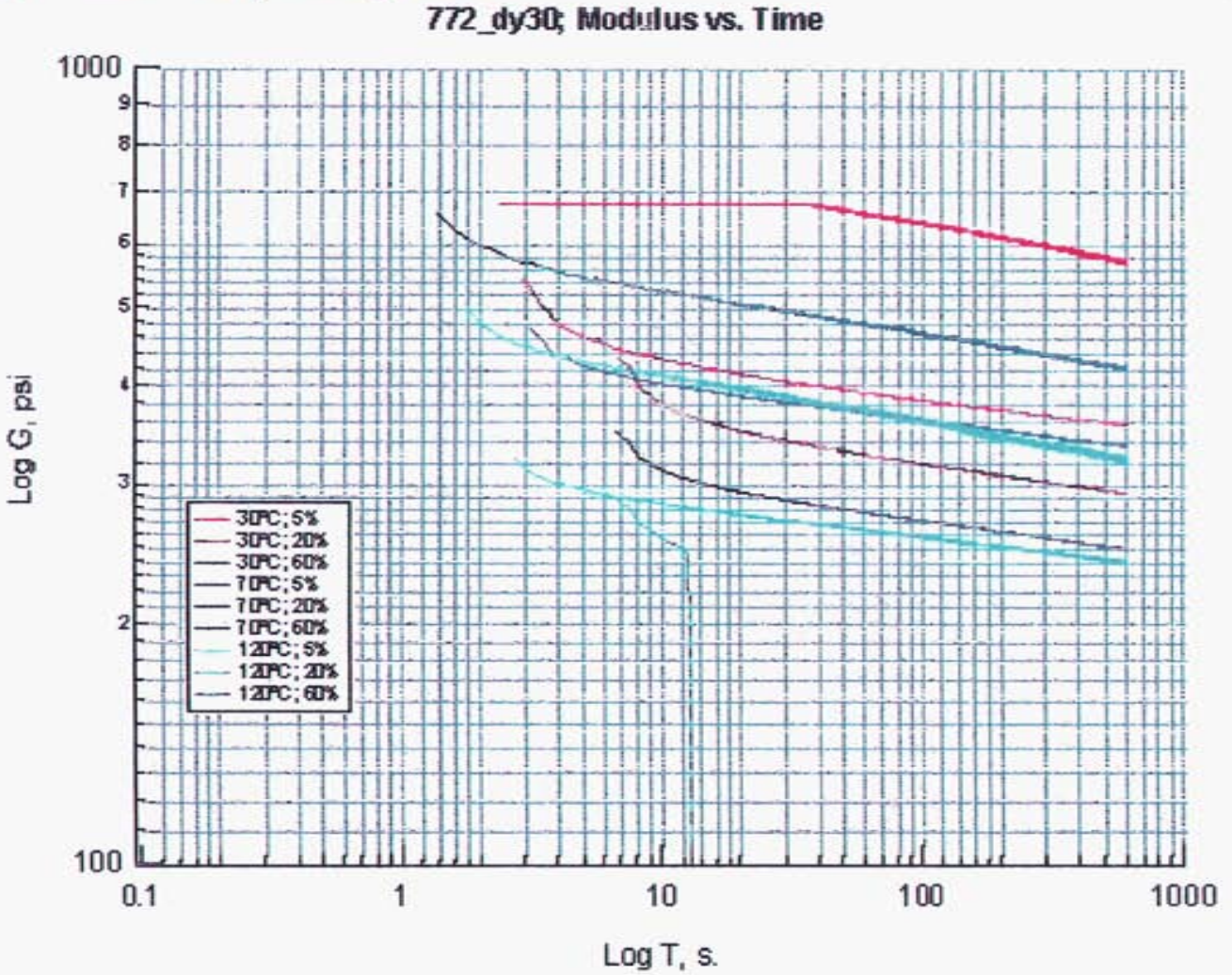

Fig. 8

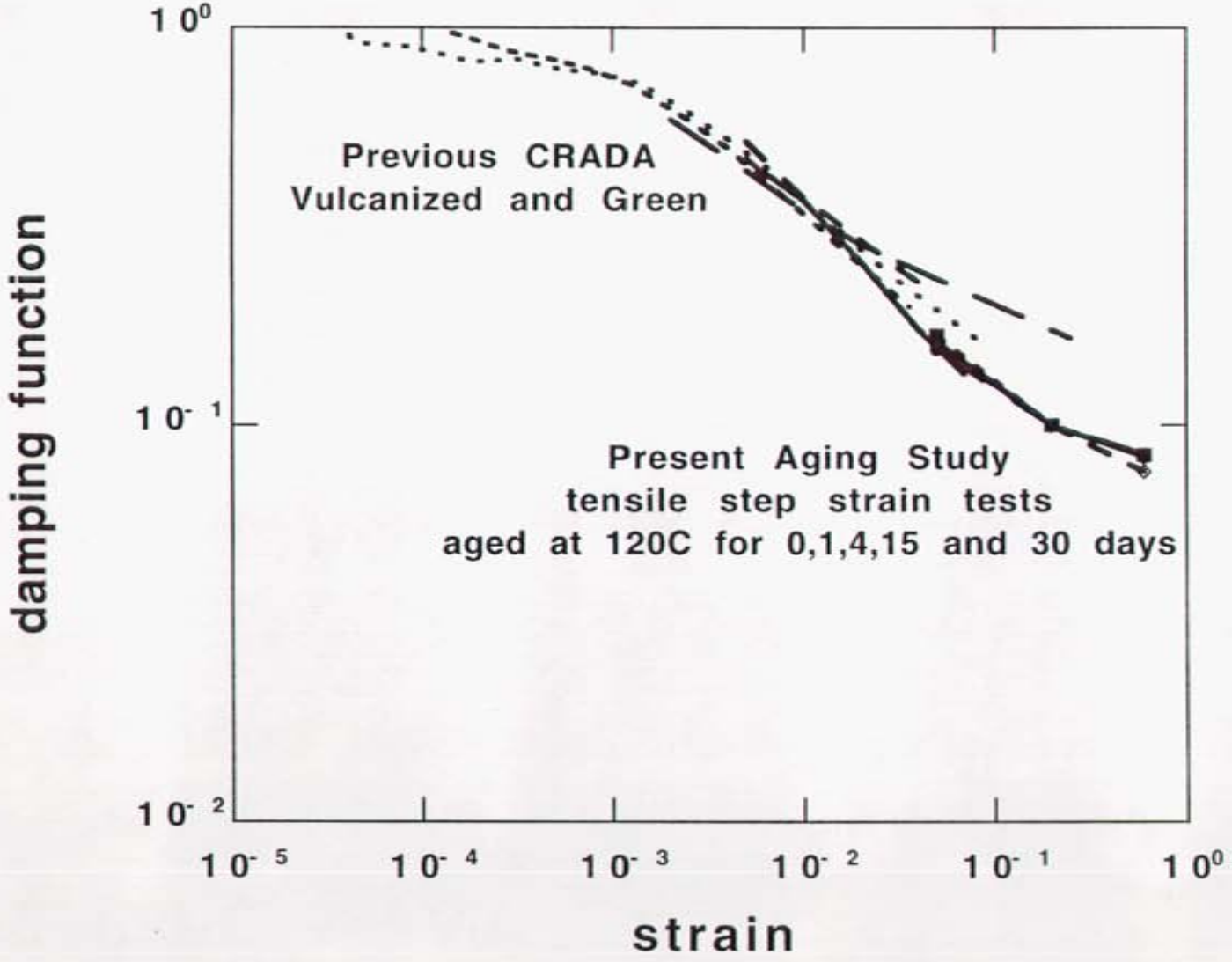
1 0^0
1 0^-1
1 0^-2
damping function
Previous CRADA
Vulcanized and Green
Present Aging Study
tensile step strain tests
aged at 120C for 0,1,4,15 and 30 days
1 0^-5
1 0^-4
1 0^-3
1 0^-2
1 0^-1
1 0^0
strain

Fig. 9

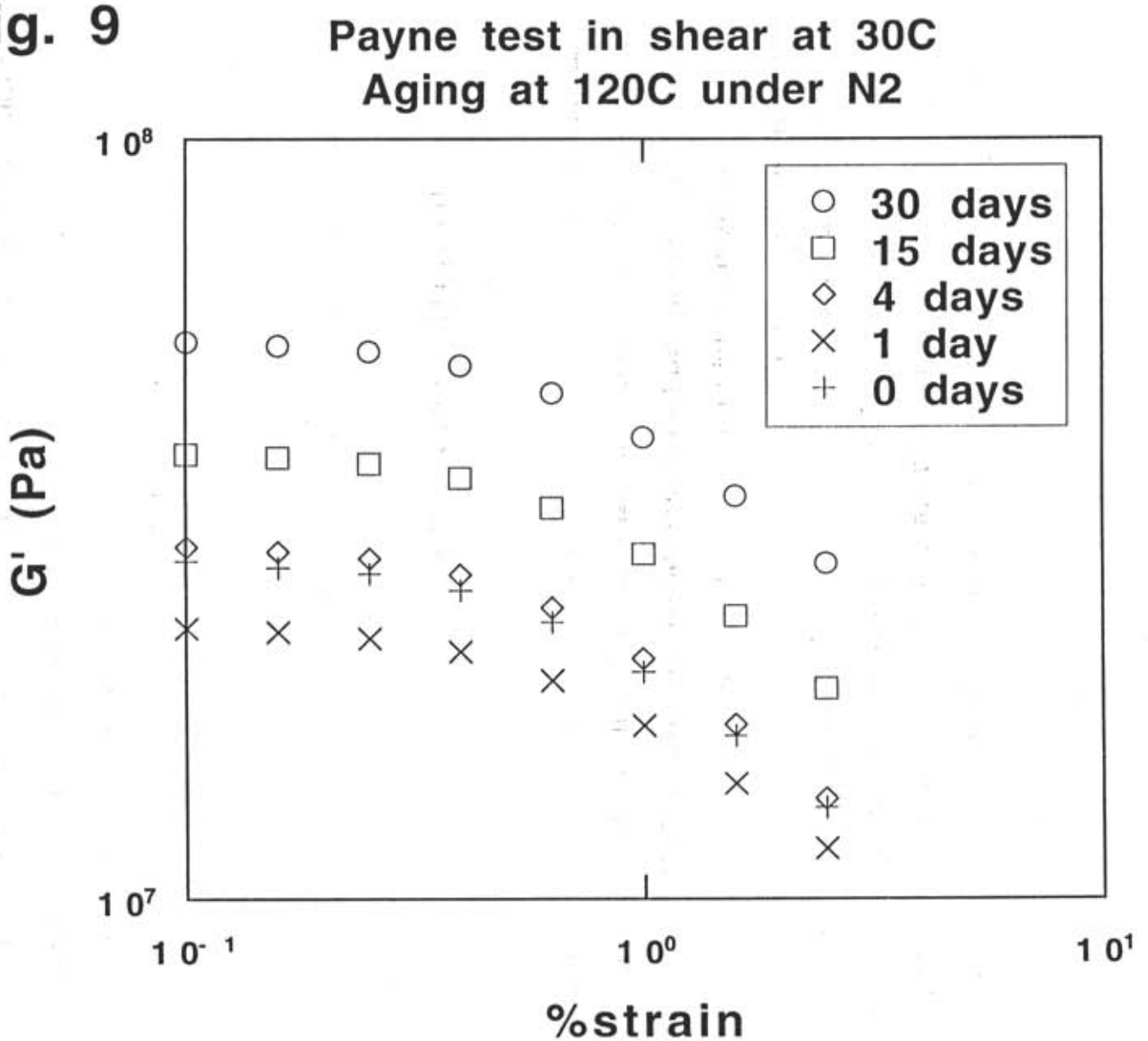
Payne test in shear at 30C
Aging at 120C under N2
1 0^8
1 0^7
G' (Pa)
1 0^-1
1 0^0
1 0^1
%strain
30 days
15 days
4 days
1 day
0 days

Fig. 10

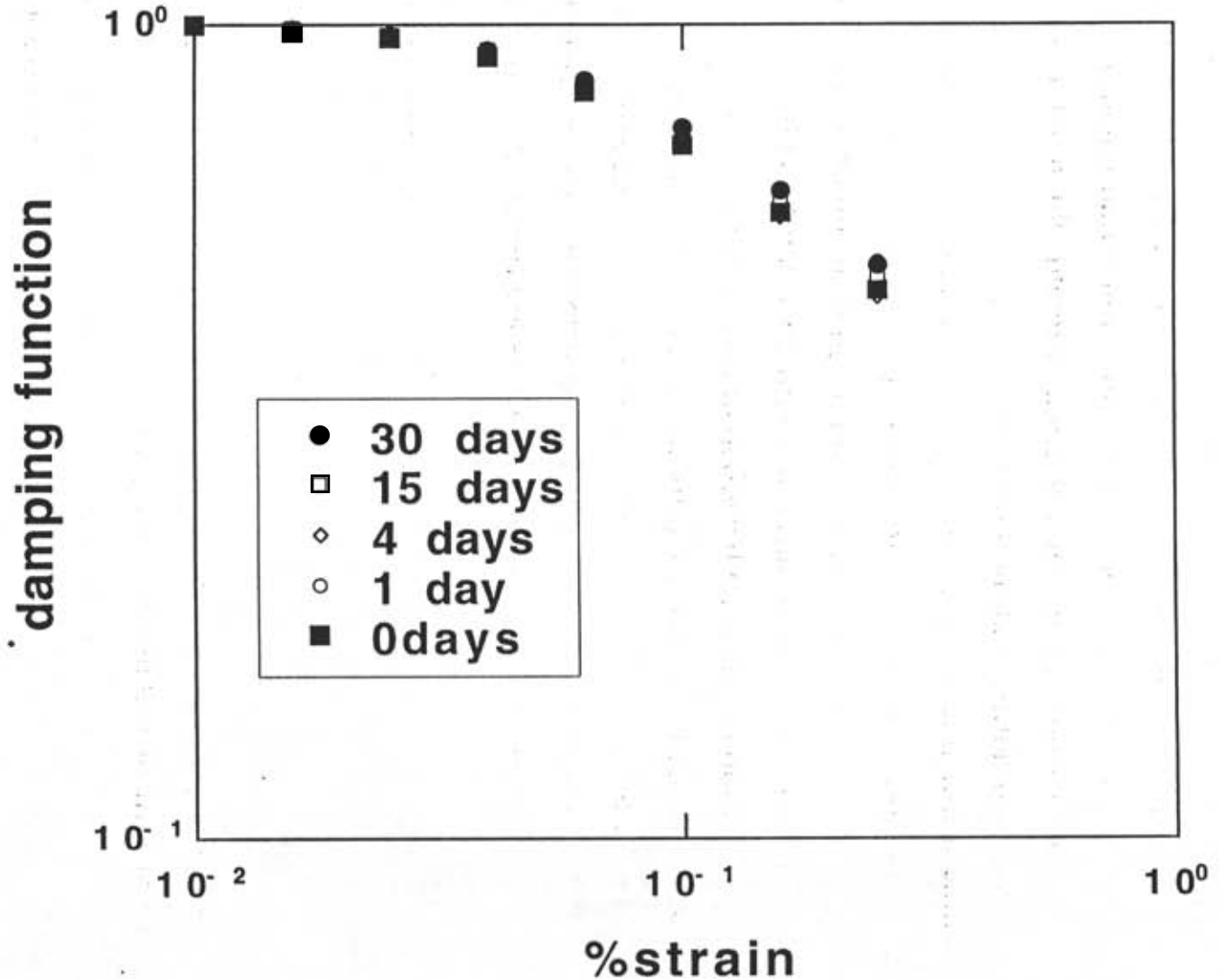
1 0^0
1 0^-1
1 0^-2
1 0^-1
1 0^0
damping function
%strain
30 days
15 days
4 days
1 day
0days

Fig. 11

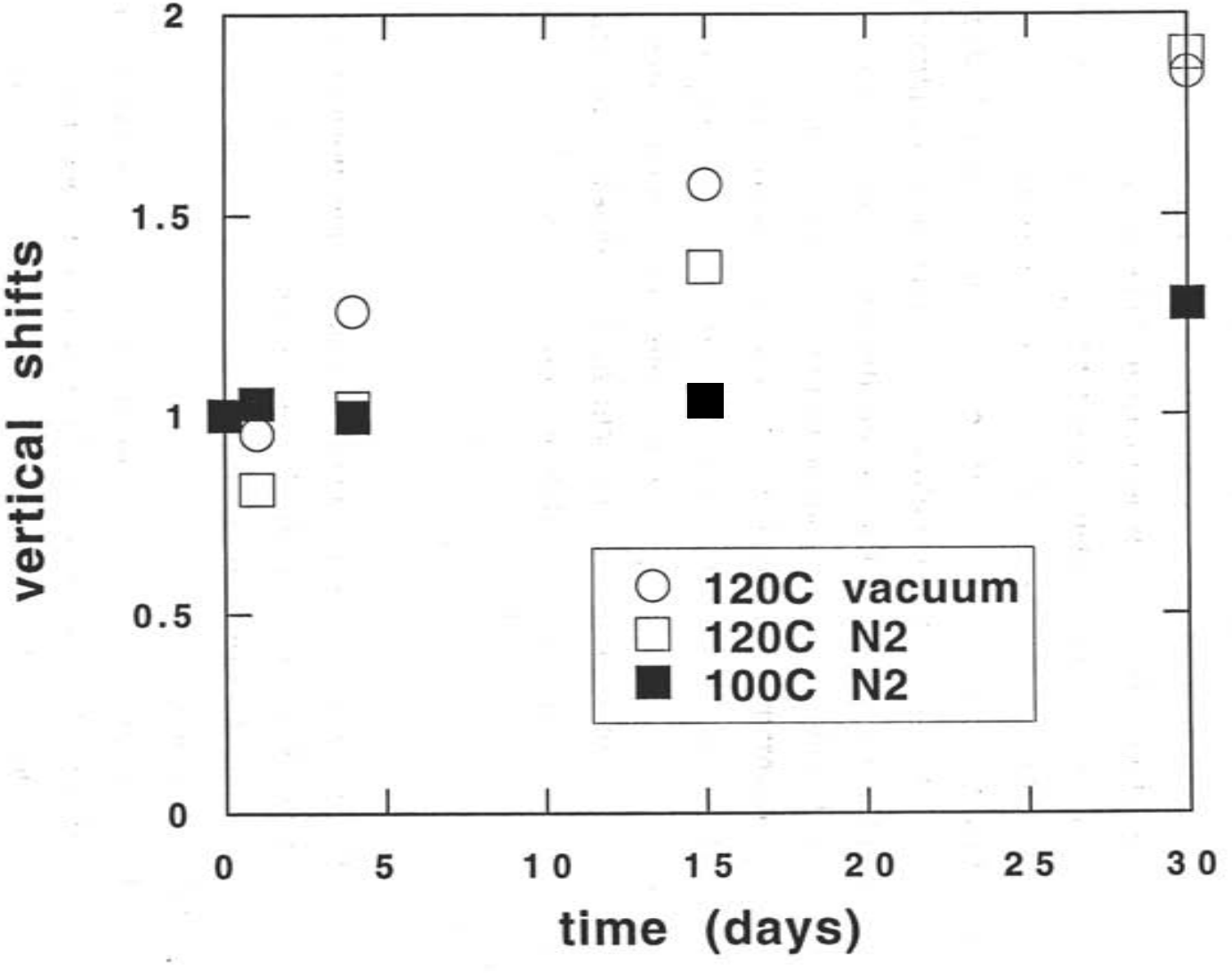
vertical shifts
2
1.5
1
0.5
0
0
5
10
15
20
25
30
time (days)
120C vacuum
120C N2
100C N2

Fig. 12

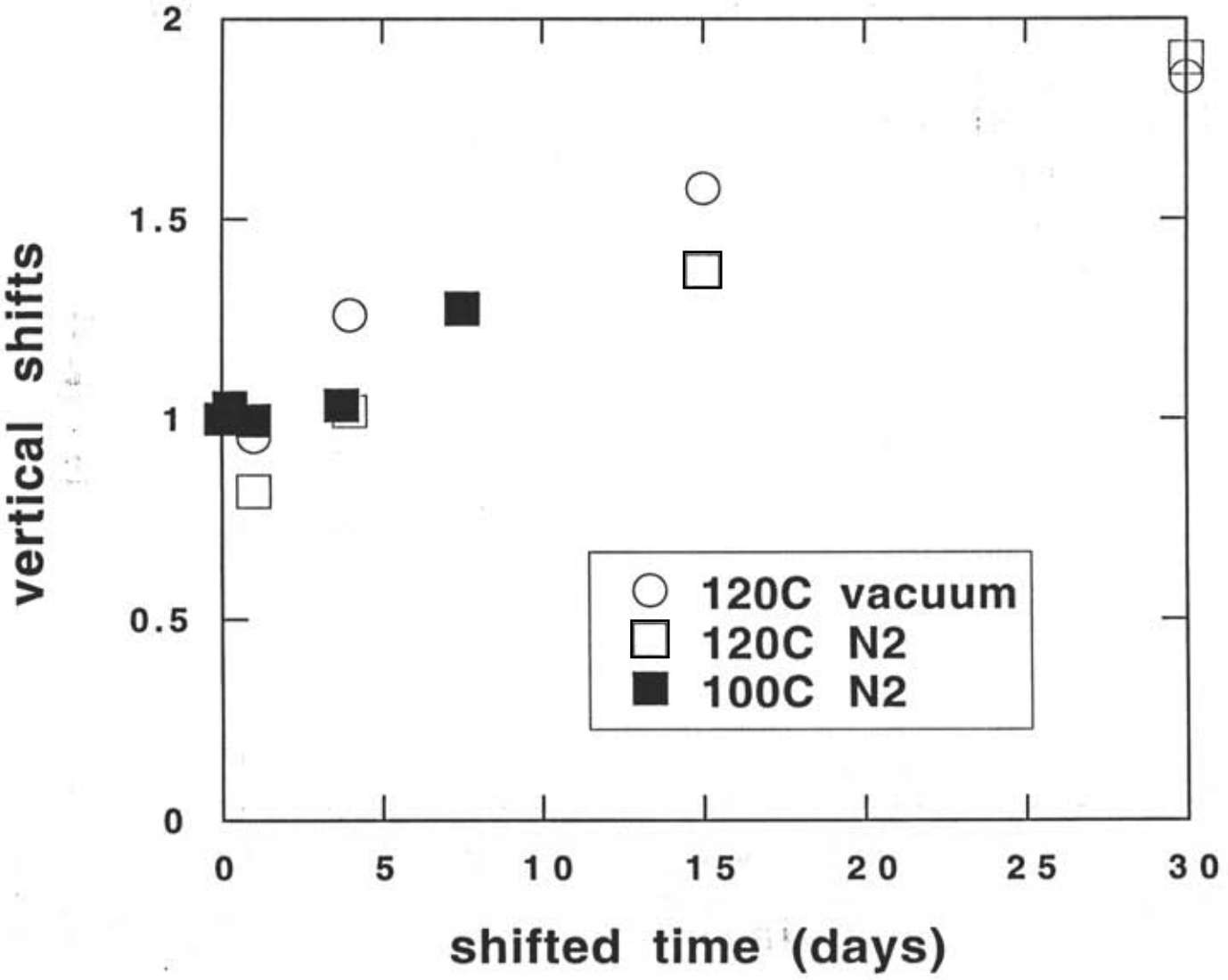
vertical shifts
shifted time (days)
0
0.5
1
1.5
2
0
5
10
15
20
25
30
120C vacuum
120C N2
100C N2

frequency but increasing magnitude. In Fig. 9, we show the dynamic storage moduli from these Payne tests on samples aged 0, 1, 4, 15, and 30 days at 120C. We showed previously that the normalized G′ is a fair approximation to the BKZ damping function at low strains.[4] In Fig. 10, we show these normalized storage moduli for all aging times. It is very clear that the damping function at low strains is also unaffected by chemical aging. As a note, these particular nonlinear tests were conducted in torsional rectangular geometry which, while increasing our torque signal, enforces a nonuniform strain field on the rubber. Therefore, while the changes between samples can be directly compared, these "damping functions" cannot be directly compared to the true damping functions obtained from step strain tests.

Since all of the linear viscoelastic relaxation moduli were seen to superpose and strain separability held true, we can parameterize the effects of aging under no strain by a vertical shift. If more crosslinks are broken than formed, the material will soften and we apply a downwards vertical shift to the data curves. These vertical shifts are therefore a function of aging time and reflect the balance between formation and scission of crosslinks as time progresses. In Fig. 11, we show these vertical shifts for rubbers aging at 100 and 120C. Again, we see the influence of an incomplete anaerobic environment in that the samples harden over a month's time.

However, we do observe that the 100C samples age slower as expected. In Fig. 12, we superpose the 100 and 120C aging curves by shifting the 100C data to lower times; that is, the 100C sample ages less in a given time than does a 120C sample. Since we shifted by a factor of four, we have followed the old rule of thumb that the reaction rate doubles every 10C. This leads to an activation energy of roughly 20 kcal/mole

which is again consistent with the observations of Gillen.

*Implications for a Constitutive Equation*

It would seem that the BKZ formalism applies with little change except to include this vertical shift. Unfortunately, the aforementioned vertical shift is extremely bothersome. We have assumed to this point that the chemistry, and therefore the vertical shifts, are due to changes in the total crosslink density. The crosslink density only enters Eq. 1 in the rubbery modulus, $G_\infty$, and we observed in Fig. 12 about a factor of two increase in the total number of crosslinks (i.e. $G_\infty$) with age. The strain softening, in contrast, enters only in the decaying term and, in Fig. 8, we see that the rubbers strain soften by an order of magnitude. The lore states that, at high strains where the rubbery modulus dominates, the carbon black network is destroyed and the black acts only as inert "hard balls" without strain softening.

We have a conceptual problem if we enforce both that the crosslinks increase by a factor of two and the sample softens by an order of magnitude at all aging times. Return to the linear viscoelastic behavior shown in Fig. 2. Here, the modulus of the sample aged 30 days is roughly twice that of the unaged sample (an increase from ~20 MPa to ~40MPa). If we attribute this increase to only the rubbery modulus, then the rubbery modulus of the 30 day sample must be roughly 20 MPa. But if this were true, the 30 day sample could not strain soften by an order of magnitude. Instead, it would only decrease until it reached the underlying rubber modulus (a factor of two decrease). One path out of this conundrum lies in insisting that both the rubbery and decaying terms in Eq. 1 are proportional to the crosslink density. In this fashion, as the crosslink density increases by

a factor of two, the decaying term increases by a factor of two. The rubbery modulus alone need not cause this increase; it can still be an order of magnitude lower, which allows us room to strain soften by the required order of magnitude.

What physical picture does this imply that is consistent with the lore? Perhaps the carbon black network is not simply pictured as interacting adjacent black particulates but, instead, particulate interaction is mediated by absorbed polymer. The strain softening could arise from de-adhesion of the polymer from the black or nonlinear viscoelastic "untangling" of absorbed polymer on adjacent black particulates. The dependence of this softening on chemistry, then, could arise from the "hardening" of these interacting absorbed layers by an increase in crosslink density or perhaps be a reflection of increased adhesion by intrinsic surface chemistry. From a phenomenological nonlinear viscoelastic perspective, we are not terribly concerned with the details of the underlying chemistry. Rather, we understand that we need to incorporate the effects of chemical aging directly into the appropriate nonlinear viscoelastic constitutive formalism.

## IV. AGING UNDER STRAIN

*Test Data*

Our second series of studies considered the effect of chemical aging under a constant applied strain. Here, the force required to maintain this constant strain will be sensitive to only those crosslinks that are broken. Special tension jigs were made that maintained a given tensile strain in the vacuum oven. The samples were aged in the vaccum oven following the same aging protocol at 100 and 120C under a strain of 20%. At intervals of 1, 4, 15, and 30 days, a jig was removed from the oven, fixtured in an

Instron, and the force required to maintain the 20% strain was measured. Since considerable decay occured in just the first day, we also measured the initial tensile stress relaxation with an Instron for 4 hours in air at 100 and 120C. From the continuity of the two data sets, it appears that not much oxidative decay occurs during this short initial period. This experimental procedure is somewhat non-standard so more detail is given in Appendix 1.

At both 100 and 120C, the force required to maintain a 20% strain decreased rapidly with time. As seen in Fig. 13, the force dropped to half of the initial value in only a couple of days. The 120C decay, of course, was steeper than the 100C decay due to accelerated degradation kinetics at the higher temperature. We can again superpose the two curves (Fig. 14) by shifting the 100C data by the same factor of four used in Fig. 12 implying that the degradation kinetics have an activation energy of roughly 20 kcal/mole. Since this is the same activation energy governing the total crosslink density, we conclude that the formation and scission reactions have about the same activation energy.

It is important to note that after these samples were tested and removed from the clamping fixtures, they did not return to their original unstrained length but maintained a permanent elongation even after high temperature annealing. In the analogous compressive experiments on aging rubbers, this effect is well-known as compression set and reflects the complicated bookkeeping required for tracking the reference states of newly formed crosslinks.

*Implications for a Constitutive Equation*

In Fig. 15, we compare the relative changes in total crosslink density at 120C in Fig. 11 with the relative force decay due crosslink scission in Fig.

Fig. 13

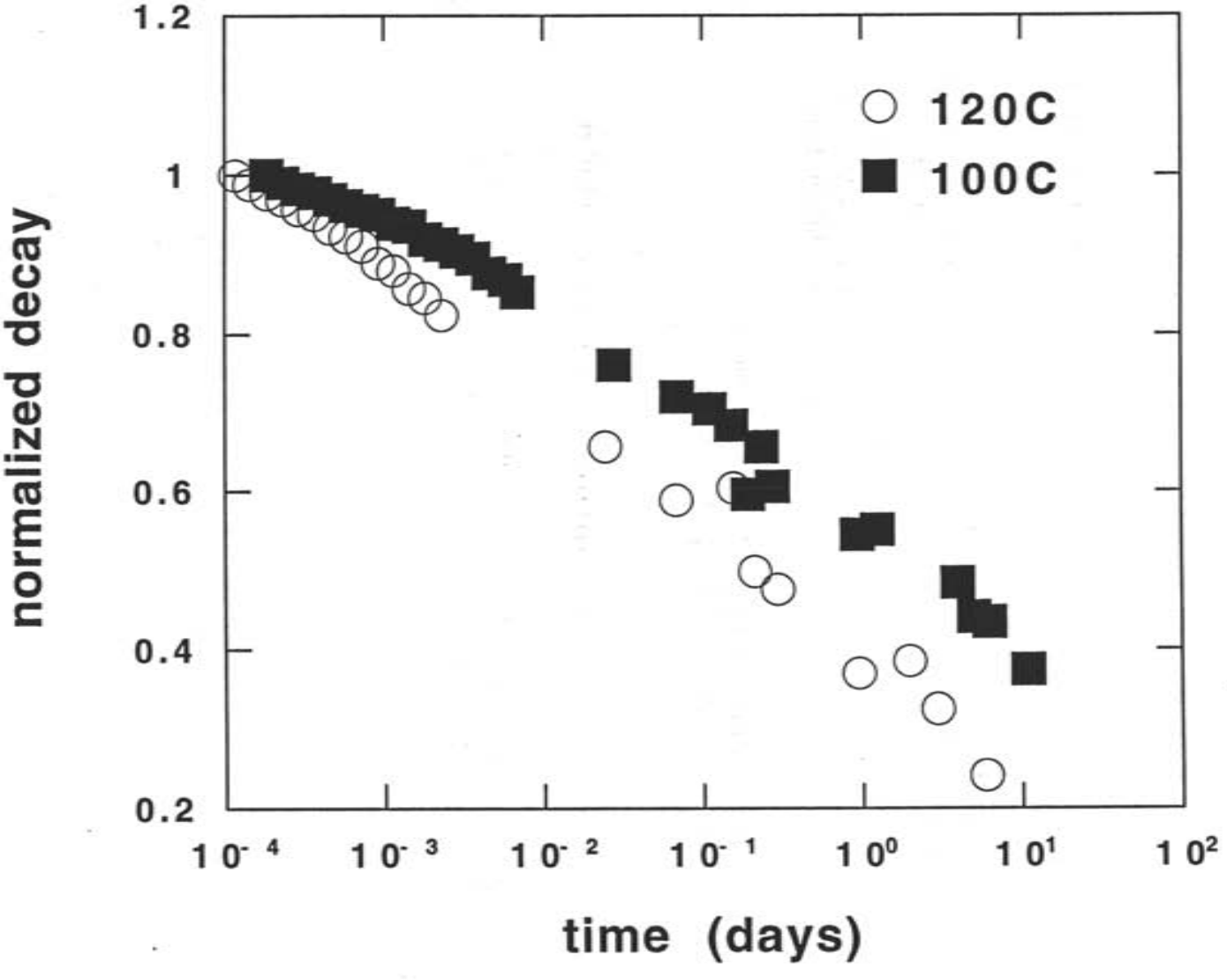
1.2
1
0.8
0.6
0.4
0.2
normalized decay
120C
100C
10- 4
10- 3
10- 2
10- 1
10 0
10 1
10 2
time (days)

Fig. 14

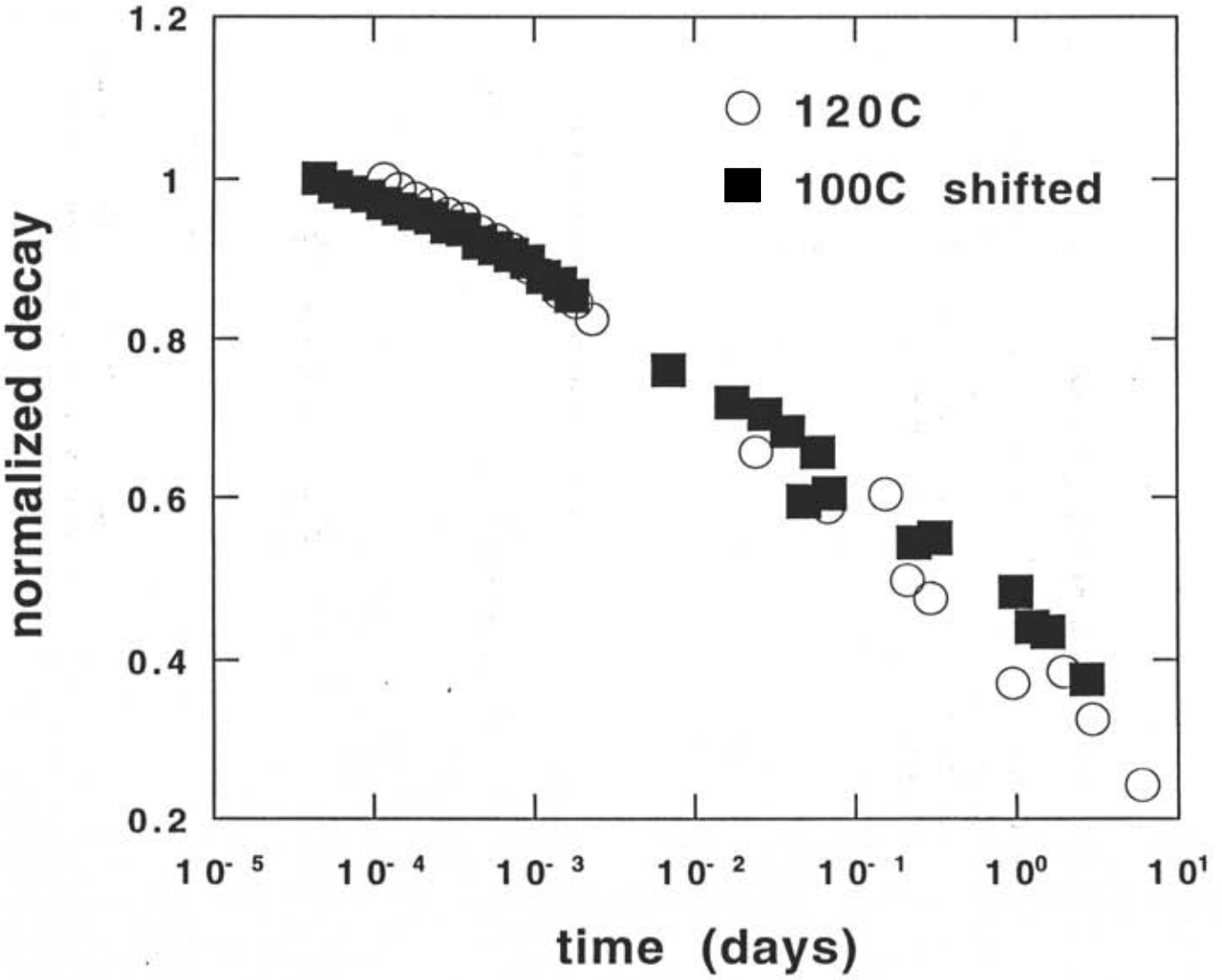
1.2
1
0.8
0.6
0.4
0.2
normalized decay
120C
100C shifted
10- 5
10- 4
10- 3
10- 2
10- 1
100
101
time (days)

Fig. 15

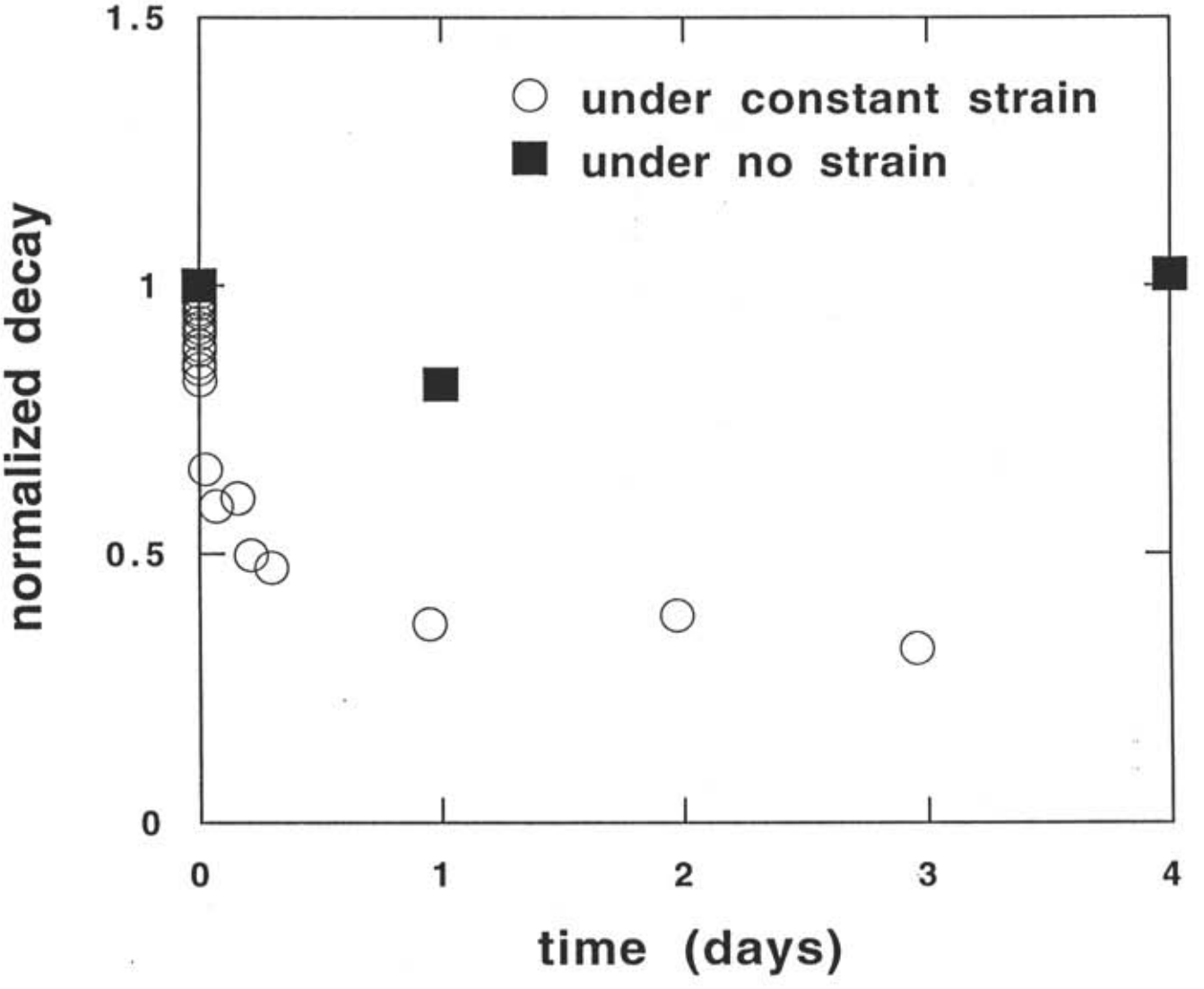
1.5
1
0.5
0
normalized decay
under constant strain
under no strain
0
1
2
3
4
time (days)

13. A dramatic difference in time scale is seen between the two tests and, and if one were not careful to perform both tests, different physical pictures could emerge. For example, if we only examined the change in total crosslink density as the sample ages by performing a simple "modulus" test, one might conclude that (a) not much chemistry actually takes place and (b) it happens fairly slowly (i.e. over a month or so).

However, the combined tests give a much different picture. Since the decay in the force required to maintain the 20% strain occurs so rapidly and decays to such a low value, it implies that a tremendous amount of chemical scission is on-going. However, since the total crosslink density is relatively level over the same period, an equal amount of crosslink formation must be occurring. Therefore, chemical reaction is rampant throughout the sample, but it just happens that about as many crosslinks are formed as are broken. This important conclusion is unchanged by the oxidation in the system seen in Fig. 1. This is a profound point in terms of the system's mechanical response, since two systems with constant total crosslink density can behave completely differently if that constant crosslink density arises from different mechanisms, e.g. a lack of any chemistry or a balance between rapid formation and scission reactions. This effect must be incorporated into our constitutive formalism.

Moreover, if the chemistry is occurring under strain, we must properly account for the reference strain of each new crosslink formed since this gives rise to compression set. For an elastic material, Segalman developed a differential model that captures the relevant physics. His memo deriving this equation is reproduced in Appendix 2. The main result is captured by

$$\frac{d\underline{\underline{\sigma}}}{dt} + \frac{\nu_b}{p}\underline{\underline{\sigma}} = 2kT\,p\,\frac{d\underline{\underline{\gamma}}}{dt} \tag{7}$$

where $\nu_b$ is the rate of crosslink scission and p is the total crosslink density. Crosslinks are formed, $\nu_f$, and broken, $\nu_b$, according to

$$\frac{dp}{dt} = \nu_f - \nu_b \tag{8}$$

Let's examine Eq. (7) for the effects of compression set. At t=0, we instantaneously stretch the sample to $\bar{\gamma}$. As it sits in this stretched state from t=0 to t=$\bar{t}$, crosslink chemistry occurs. At t=$\bar{t}$, the stretching force is released and the sample springs to a new strain which will depend on the chemistry that has taken place. Eq. (7) predicts

$$\frac{\bar{\gamma} - \gamma(t)}{\bar{\gamma}} = \frac{p(0)}{p(\bar{t})}\exp\left(-\int_0^t ds\,\frac{\nu_b(s)}{p(s)}\right) \tag{9}$$

If an equal number of crosslinks break as form

$$\frac{\bar{\gamma} - \gamma(t)}{\bar{\gamma}} = e^{-p_b/p} \tag{10}$$

where $p_b$ is the number of crosslink broken from t=0 to $\bar{t}$. If no crosslinks break, then $\gamma(t)=0$ and the sample springs back to its original, unstrained configuration as it should. If the number of crosslinks broken is much larger than the total, $\gamma(t)=\bar{\gamma}$ and the sample does not spring back at all,

again as it should. These effects described here for an elastic material must be present in the nonlinear viscoelastic material as well.

## V. CONSTITUTIVE EQUATION

The experimental results in Section III indicated that the decaying stress must be proportional to the crosslink density. The results in Section IV indicated that we must properly decouple the formation and scission reactions and carefully track their reference strains. Let's examine how these results could be implemented within the damage-based constitutive formalism. Rewriting Eqs. (2) and (7) for the decaying and equilibrium stresses respectively, we obtain

$$\underline{\underline{\sigma}} = \sum \underline{\underline{\sigma}}_i + \underline{\underline{\sigma}}_\infty$$

$$\frac{d\underline{\underline{\sigma}}_i}{dt} + \frac{1}{\tau_i}\underline{\underline{\sigma}}_i = 2\left[G_i\, g(d)\right]\underline{\underline{\dot{\gamma}}} \qquad (11)$$

$$\frac{d\underline{\underline{\sigma}}_\infty}{dt} + \frac{\nu_b}{p}\underline{\underline{\sigma}}_\infty = 2\left[kT\, p\right]\underline{\underline{\dot{\gamma}}}$$

As of yet, the decaying term does not properly reflect the necessary crosslink dependence. However, we can clearly see an analogous structure to the decaying and equilibrium stresses and a path to reconcile them.

We hypothesize that

$$\underline{\underline{\sigma}} = \sum \underline{\underline{\sigma}}_i + \underline{\underline{\sigma}}_\infty$$

$$\frac{d\underline{\underline{\sigma}}_i}{dt} + \left(\frac{1}{\tau_i} + \frac{\nu_b}{p}\right)\underline{\underline{\sigma}}_i = 2\left[\left(G_i + a_i kTp\right) g(d)\right] \underline{\underline{\dot{\gamma}}} \qquad (12)$$

$$\frac{d\underline{\underline{\sigma}}_\infty}{dt} + \frac{\nu_b}{p}\underline{\underline{\sigma}}_\infty = 2\left[kT\, p\right] \underline{\underline{\dot{\gamma}}}$$

What are the qualitative features of this approach? First, for a chemically stable system, we limit to the green rubber (i.e. p=0) and the fully cured rubber (for which $a_i kTp >> G_i$) each with their own appropriate relaxation spectrum (determined by the respective prefactors $G_i$ and $a_i$). As it cures, the relaxation spectrum naturally evolves as seen experimentally.[3] In a chemically aging system, both the decaying and equilibrium terms depend on the chemistry and reflect the interplay of the chemistry and strain histories as required by the results of Sections III and IV above.

Let's examine the results of this equation for the two types of tests that we performed on highly cured systems for which $a_i kTp >> G_i$. First, examine aging under no strain. Crosslink formation and scission occurs from $t=-\bar{t}$ to t=0 at which time an infinitesimal step strain of magnitude $\bar{\gamma}$ is applied and the stress decay is monitored. Since we monitor the stress decay for a relatively short period of time only to gain a "snapshot" of the relaxation spectrum at this aging time, we can safely assume that no appreciable chemistry occurs during the actual measurement of the relaxation spectrum. For this case, Eq. (12) predicts

$$\underline{\underline{\sigma}}(t) = 2[p(0)\,kT]\left[1 + g(d)\,\Sigma a_i\,\exp\left(-\frac{t}{\tau_i}\right)\right]\underline{\underline{\gamma}}$$

$$\text{where}\quad p(0) = p(-\bar{t})\,\exp\left(-\int_{-\bar{t}}^{0} ds\,\frac{\nu_b(s)}{p(s)}\right) \tag{14}$$

We see that the stress decays in time due to viscoelastic relaxation only. The relaxation function and damping function are invariant with cure, and the stress magnitude is determined by the total crosslink density at the time of the step strain. This result is in agreement with the experimental observations in Section III.

Now examine aging under a constant applied strain. Here, the step strain is applied at t=0 and then held constant. As time progresses, we measure the stress required to hold the sample at this strain. Crosslink formation and scission occurs throughout the test. Eq. (12) now predicts

$$\underline{\underline{\sigma}}(t) = 2[p(t)\,kT]\left[1 + g(d)\,\Sigma a_i\,\exp\left(-\frac{t}{\tau_i}\right)\right]\underline{\underline{\gamma}}$$

$$\text{where}\quad p(t) = p(0)\,\exp\left(-\int_{0}^{t} ds\,\frac{\nu_b(s)}{p(s)}\right) \tag{15}$$

We now see that the stress decays by two mechanisms, either viscoelastic relaxation or loss of crosslinks by scission [i.e. p(t)]. Since we have seen in the previous section that a significant fraction of crosslinks are broken over the course of this experiment, this second path dominates and this second test is a fairly direct method of measuring crosslink scission. Again the predictions of Eq. (12) are consistent with experiment.

## VI. CONCLUSIONS

*Implications for Tire Durability*

The proposed formalism makes several statements concerning tire durability. First, and most obvious, the stress at a particular point in an aging tire is not just a function of the applied strain, but is tightly coupled to the chemistry. By design, the chemistry in our two tests was identical by design. In the first set of tests where we aged under no strain and subsequently measured the relaxation spectrum at a constant strain, our sample's modulus *increased*. In the second set of tests where we aged under a constant strain, the load required to hold the sample at this constant strain *decreased* by almost an order of magnitude. This difference reflects a tight coupling between the strain history and the chemistry. Therefore, we cannot simply understand the stress at a point in the tire by a single measurement of, for example, the total crosslink density. We must, instead, track the detailed interplay between strain and chemistry and its effect on stress throughout the history of the tire element.

Even more detailed measurements of the crosslink distribution at a given aging time by selective scission/swelling techniques still give only "snapshots" of the total crosslink density and do not reflect this coupling between chemistry and strain history. Suppose we had a rubber for which the rates of formation and scission were equal for each crosslinking species. We would observe no change in the crosslink distribution but, yet, a tremendous amount of chemistry could be taking place. While this rubber's crosslink distribution would appear similar to that for a chemically inert rubber, the stresses in these two rubbers within a tire would be completely different as they age. To understand the stress at a

particular location within a tire, we cannot just measure even the crosslink distribution at a given aging time, but once again need to track now the even more detailed interplay between the history of strain and chemistry.

How does this tight coupling affect tire durability calculations? Let's assume that we are able to correlate the growth rate of a fatigue crack with the instantaneous crosslink distribution in well-defined lab tests. That is, we are assuming that we can predict the distance a crack would grow if we knew the stress and strain fields near the crack and the current crosslink density (this is a BIG assumption). This obviously necessitates an accurate calculation of the stresses and strains in a tire to predict durability. We have shown, though, that the actual stress and strain at a point in a tire are not simply dependent on the current crosslink density but can only be calculated by tracking the coupled strain and chemical histories. Therefore, even though we may be able to correlate fatigue crack growth with instantaneous crosslink density in lab tests, we need to track the formation and scission chemical histories in a tire to predict the stresses and strains upon which our correlation was based.

*Need for Refined Degradation Chemistry Models*

The conclusions above imply the need to understand the crosslink chemistry more clearly in these systems. We need to track not only the total crosslink density changes but the individual rates of formation and scission. Moreover, it may be necessary to understand not only the total formation and scission kinetics but the individual mono-, di-, and poly-sulfidic linkage kinetics. This level of understanding goes beyond the current state-of-the-art where we, at best, track the instantaneous crosslink distribution.

To uncover these species rates, it would, at least, be necessary to

perform the "no strain/constant strain" tests on samples with differing crosslink distributions to uncouple the individual species formation and scission rates. This may be quite difficult given the extreme sensitivity to oxygen observed in our experiments.

## VII. ACKNOWLEDGEMENTS

We would like to thank Goodyear for pursuing the differences between the aging of our samples and those from inside tires which uncovered the presence of oxidative aging.

## APPENDIX 1

Typical specimen dimensions:

W = 0.185" (4.7 mm)
T = 0.083" (2.1 mm)
L = 1.183" (30 mm)

Step 0: Precondition the material in vacuum (29.2" Hg) for a week.

Step 1: Guided by the jig, which provides consistent alignment and gage length, the grips are locked in place and the specimen is put in position.

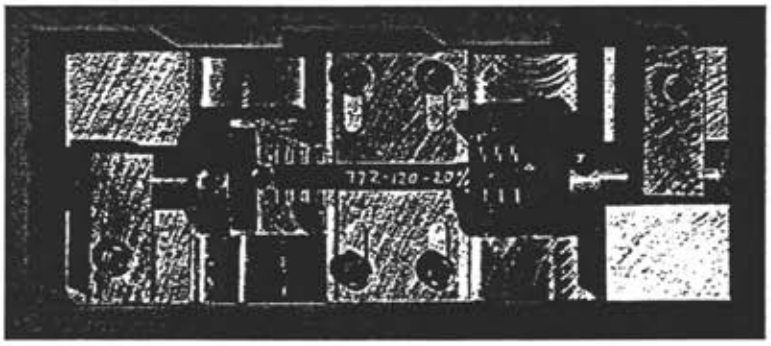

Step 2: Tighten the grips.

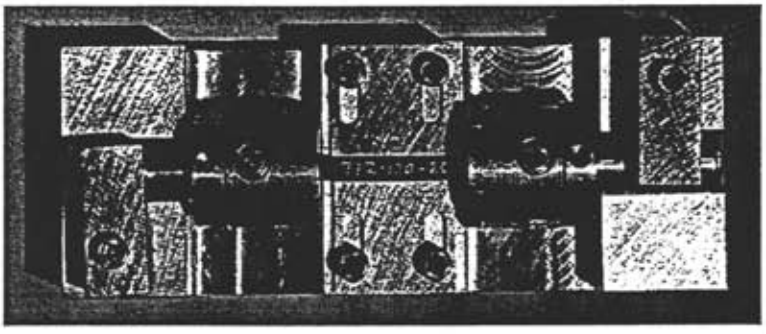

Step 3: Install the "backbone", so the specimen and grips assembly is not disturbed when transferring to the loading system.

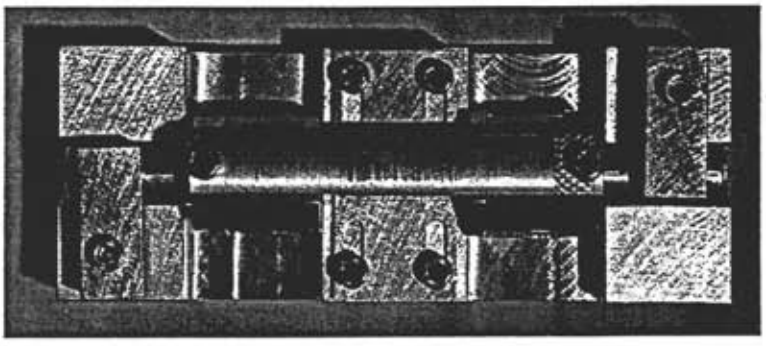

Step 4: Mount the assembly on the loading system. The environmental chamber is at elevated temperature.

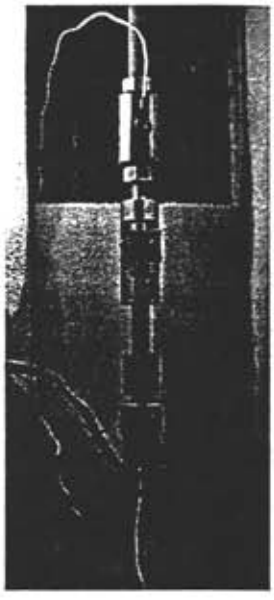

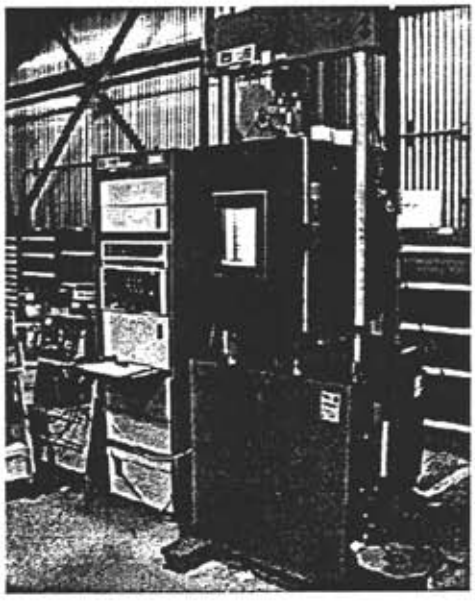

Step 5: Remove the "backbone" and loosen the bottom grip. Wait for 10 min, retighten the bottom grip; the specimen is ready for loading.

Step 6: The actuator moves a prescribed distance. After recording the initial relaxation, a spacer is inserted between grips to maintain a constant deformation of the specimen.

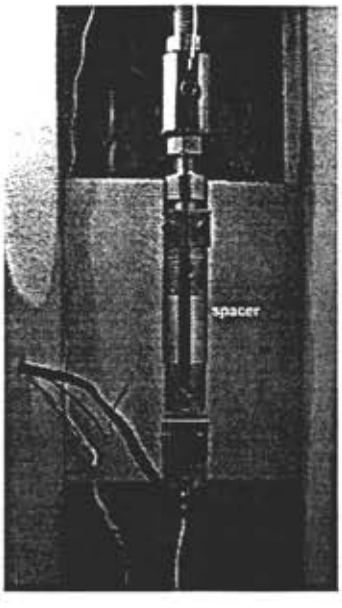


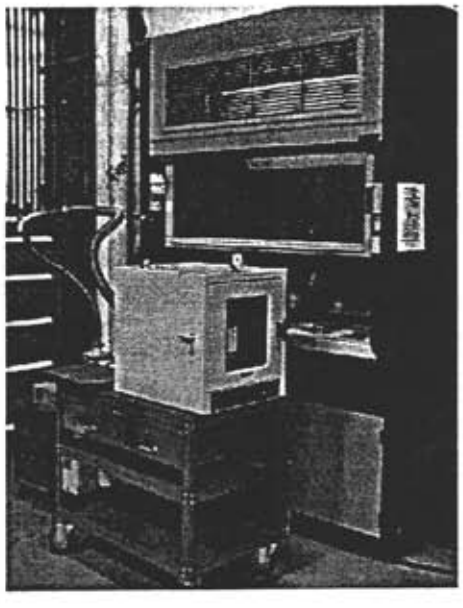

Step 7: The specimen-grips-spacer assembly is placed in a vacuum oven at elevated temperature.

Step 8: The oven is vacuumed to 29.5" Hg then back filled with nitrogen. The vacuum-and-back fill process repeats three times. Industrial grade nitrogen is used. Typical oxygen content is 50 ppb (parts per billion); maximum oxygen content is less than 100 ppb.

Step 9: When measuring relaxation load, the specimen-grips-spacer assembly is removed from oven and mounted on the loading system in the environmental chamber, which is at elevated temperature.

Step 10: Gradually increase the stroke at a very slow rate ($10^{-4}$ in/s) till load-displacement curve bends. Remove the assembly from the loading system and put it back in the oven. Repeat Step 8.

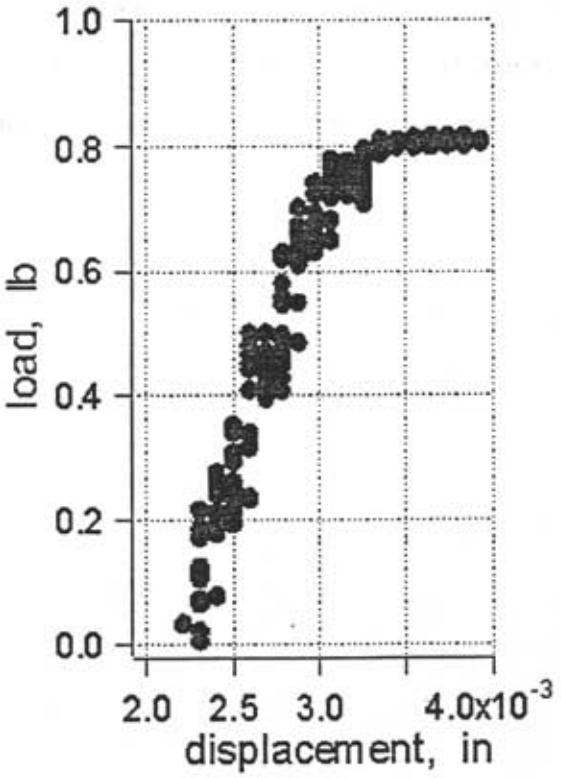

**Appendix 2**

Sandia National Laboratories

Albuquerque, New Mexico 87185

date: April 30, 1997

to: Distribution

from: Dan Segalman, 9234

subject: Calculation of Long-Term "Elastic" Stress

Following is a simplistic approach to calculating the decaying "elastic" stress in nominally elastic rubber as a result of creation and scission of crosslinks. Also presented is a formal manner to accommodate the very large temperature dependence of the apparent elastic modulus. This constitutive development shown here has undergone much evolution over the last couple of weeks; it is still in flux. I would appreciate any guidance that you could give to make this more useful and more predictive.

In this discussion, I prefer not to refer to this evolving stress as the elastic stress. A material with a changing rest state cannot be elastic. Instead, I refer to this quantity as "equilibrium stress". I am open to vocabulary suggestions also.

# Relaxation of Equilibrium Stress

As is conventionally done, we assume that the current stress is due to the contributions of all past strains weighted by the number crosslinks formed in those states that survive to the present time:

$$\frac{\sigma_\infty(t)}{kT} = \int_{-\infty}^{t} 2\mu(t,s)[\varepsilon(t)-\varepsilon(s)]ds \qquad \text{(EQ 1)}$$

where

| | |
|---|---|
| $\sigma_\infty(t)$ | is the deviatoric part of the stress equilibrium stress |
| $k$ | is Boltzman's constant |
| $T$ | is absolute temperature |
| $\varepsilon(t)$ | is the (small) strain tensor at time t |
| $\mu(t,s)ds$ | is the population (per unit volume) of cross links formed in the time interval $(s, s+ds)$ that have survived to time $t$ |

We now relate the quantity $\mu(t, s)$ to the cross link kinetics: $\nu_b$ = the rate per unit volume at which crosslinks are destroyed, and $\nu_f$ = the rate per unit volume at which crosslinks are formed. Further, we transform our constitutive equation into a differential form employing these quantities.

Let $p(t)$ be the instantaneous population of crosslinks at time $t$. By definition,

$$\dot{p}(t) = \nu_f(t) - \nu_b(t) \qquad \text{(EQ 2)}$$

We now examine $\mu(t, s)$ and its time derivative $\frac{\partial}{\partial t}\mu(t, s)$. The quantity $\mu(t, s)ds$ is the number of crosslinks formed in the time interval $(s, s + ds)$ that survive to the current time. We assume that the likelihood of any of these crosslinks breaking is the same as that of any other crosslink in the network breaking. Hence the rate of decay of this population is proportional to the overall rate of decay of crosslinks in the system and to the their presence in the population:

$$\frac{\partial}{\partial t}\mu(t, s) = -\frac{\nu_b(t)}{p(t)}\mu(t, s) \qquad \text{(EQ 3)}$$

By definition,

$$\mu(t, t) = \nu_f(t) \qquad \text{(EQ 4)}$$

We next calculate the time derivative of stress (Equation 1):

$$\frac{\partial}{\partial t}\left[\frac{\sigma_\infty(t)}{kT}\right] = 2\dot{\varepsilon}(t)\int_{-\infty}^{t}\mu(t, s)ds + \int_{-\infty}^{t}2\frac{\partial}{\partial t}\mu(t, s)[\varepsilon(t) - \varepsilon(s)]ds \qquad \text{(EQ 5)}$$

which is expressed in terms of $p$, $\nu_f$, and $\nu_b$:

$$\frac{\partial}{\partial t}\left[\frac{\sigma_\infty(t)}{kT}\right] = 2\dot{\varepsilon}(t)p(t) - \frac{\nu_b(t)}{p(t)}\frac{\sigma(t)}{kT} \qquad \text{(EQ 6)}$$

where it has been observed that $\int_{-\infty}^{t}\mu(t, s)ds = p(t)$

Lets now cast this into a form using observable parameters. We consider the case of an isothermal, step-function strain experiment: strain rate is $\dot{\varepsilon}(t) = \varepsilon_0\delta(t)$. For this experiment, Equation 6 yields:

$$\sigma_\infty(0^+) = 2\varepsilon_0(p(0)kT) \qquad \text{(EQ 7)}$$

We see that we can now identify $p(0)kT$ with $G_\infty(0)$. Also, we note that after the step function strain,

$$\dot{\sigma}_\infty(t) = -\frac{\nu_b(t)}{p(t)}\sigma_\infty(t) \qquad \text{(EQ 8)}$$

so we may associate the term $p(t)/\nu_b(t)$ with the instantaneous decay time, $\tau_\sigma$, of stress after step function strain.

The evolution equation for stress is now:

$$\frac{\partial}{\partial t}\left(\frac{\sigma_\infty}{kT}\right) + \left(\frac{\sigma_\infty}{kT}\right)/\tau_\sigma(t) = 2\dot{\varepsilon}\left[\frac{p}{p(0)}\frac{G_\infty(0)}{kT}\right] \qquad \text{(EQ 9)}$$

In general, we would still have to solve for the population, $p$, of cross-links, but for butyl rubber, some more simplification can be made. For this class of rubber, one approximates:

$$\nu_f(t) = \nu_b(t) \qquad \text{(EQ 10)}$$

so

$$\dot{p}(t) = 0 \quad \text{and} \quad p(t) = p(0) \qquad \text{(EQ 11)}$$

Equation 9 is now:

$$\frac{\partial}{\partial t}\left(\frac{\sigma_\infty}{kT}\right) + \left(\frac{\sigma_\infty}{kT}\right)/\tau_\sigma(t) = 2\dot{\varepsilon}\frac{G_\infty(0)}{kT} \qquad \text{(EQ 12)}$$

The decay time, $\tau_\sigma$, is itself parameterized by temperature and chemistry, and is found experimentally.

## Appendix 3

Simplification of the modified differential damage-like model (Eqs. 2-6) for a time-dependent simple shearing deformation [i.e. $\underline{\underline{\gamma}}_{dev_{12}} = \gamma(t)$] where all the relaxation prefactors are equal (i.e. $G_i = a_{d_i} = a_{K_i} = a_{I_i}$).

$$\underline{\underline{\sigma}} = -P\,\underline{\underline{I}} + 2G_{glassy}\int_0^t ds\; g(d(s))\, f(t-s)\, \dot{\underline{\underline{\gamma}}}_{dev}(s) + 2G_\infty \underline{\underline{\gamma}}_{dev}$$

$$d = \int_0^t ds\; f(t-s)\, \dot{D}$$

$$\dot{D} = \sqrt{2\dot{\gamma}^2}\; H(\varepsilon\dot{\gamma})\; \delta\left(\sqrt{2\varepsilon^2} - d\right)$$

$$\varepsilon = \int_0^t ds\; f(t-s)\, \dot{\gamma}(s)$$

## VIII. REFERENCES


(1) Mark Weinberg, *The Rheology of Carbon Black Filled Elastomers*, PhD Thesis, MIT, January, 1981.

(2) B. Bernstein, E. A. Kearsley, and L. J. Zapas, *Trans. Soc. Rheol.*, **VII**, 391 (1963).

(3) D. Adolf, *Rheology of Carbon Black Filled Rubber During Cure*, SAND96-1313, Sandia National Laboratories, 1996.

(4) D. Adolf, *Rheology of Green Carbon Black Filled Rubber*, SAND95-1501, Sandia National Laboratories, 1996.

(5) R. G. Larson, *Constitutive Equations for Polymer Melts and Solutions*, Butterworths, Boston, 1988.

(6) D. J. Segalman, K. Zuo, and D. Parsons, *Damage, Healing, Molecular Theory, and Modelling of Rubbery Polymer with Active Filler*, SAND95-2088, Sandia National Laboratories, 1995.

(7) J. D. Ferry, *Viscoelastic Properties of Polymers*, Wiley, NY, 1980.

(8) H. Ambacher, M. Strauss, H. G. Killian, and S. Wolff, *Kautschuk & Gummi Kunststoffe*, **44**(12), 1111 (1991).

(9) M. Gerspacher and C. P. O'Farrell, *Kautschuk & Gummi Kunststoffe*, **45**(2), 97 (1992).

(10) M.-J. Wang, S. Wolff, and E.-H. Tan, *Rubber Chem. & Tech.*, **66**, 178 (1993).

(11) A. Mallick, D. K. Tipathy, and S. K. De, *Rubber Chem. & Tech.*, **67**(5),845 (1994).

(12) G. G. A. Bohm and M. N. Nguyen, *J. Appl. Polym. Sci.*, **55**(7), 1041 (1995).

**DISTRIBUTION**

| | | |
|---|---|---|
| 1 | MS9018 | Central Technical FIles, 8940-2 |
| 5 | MS0899 | Technical Library, 9616 |
| 20 | MS0333 | Doug Adolf, 1811 |
| 1 | MS1407 | Roger Clough, 1811 |
| 1 | MS0847 | Hal Morgan, 9117 |
| 1 | MS0847 | Bob Chambers, 9117 |
| 1 | MS1407 | Ken Gillen, 1811 |
| 5 | MS0847 | Wei-Yang Lu, 8725 |
| 1 | MS0612 | Review & Approval Desk, 9612<br>FOr DOE/OSTI |
| 1 | MS1380 | Technology Transfer, 4331 |